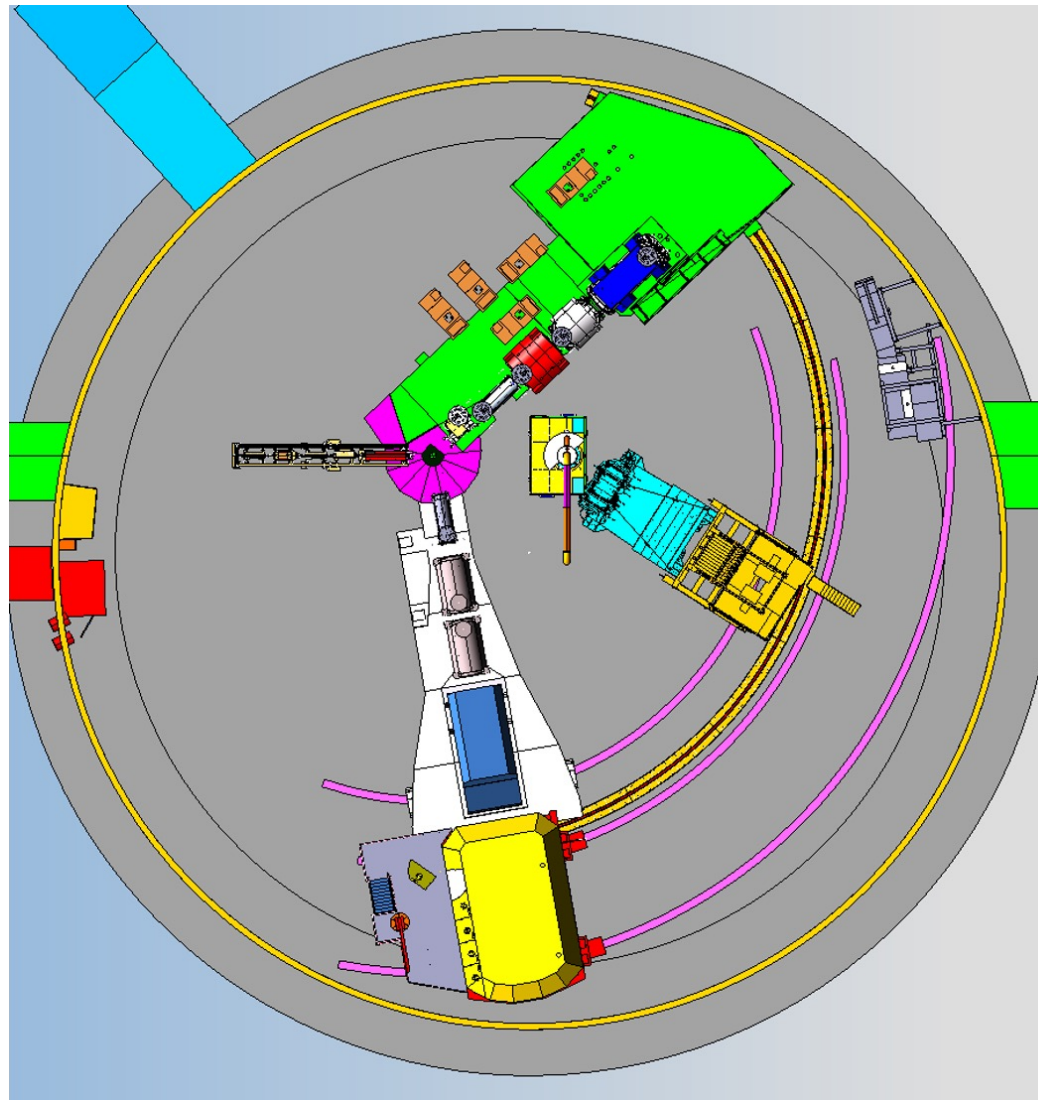


The future of SBS experiments

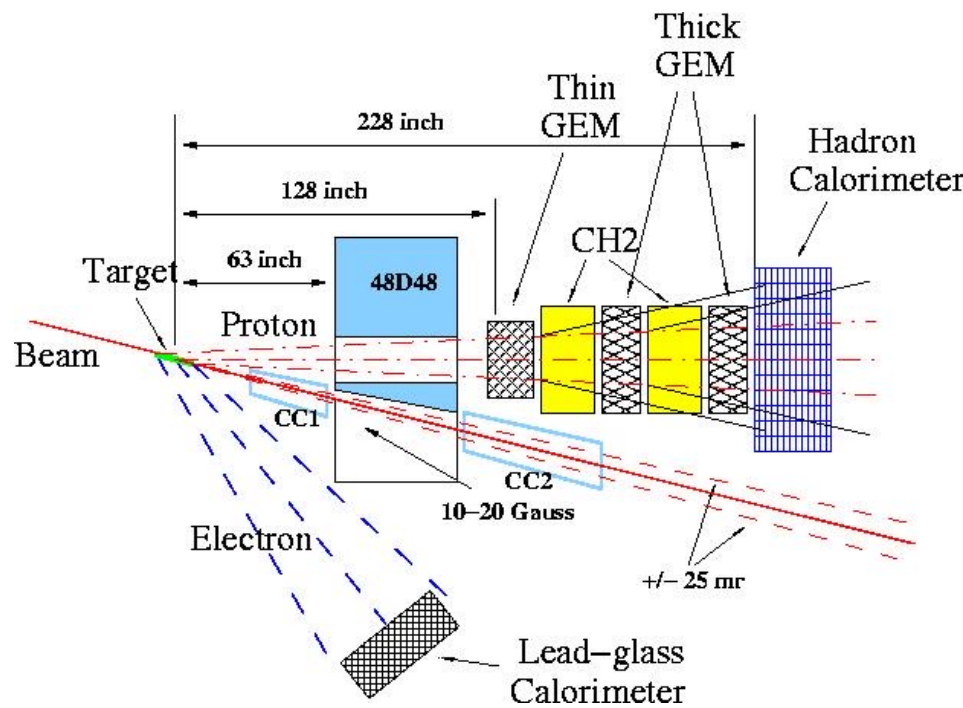
Bogdan Wojtsekhowski, for the SBS collaboration

The future of SBS is in Hall C



Experiment: Layout and Parameters

$$H(\vec{e}, e' \vec{p})$$



Beam: 75 μA , 85% polarization

Target: 40 cm liquid H_2

Electron arm at 37° , covers Q^2 range from 12.5 to 16 GeV^2

Proton arm at angle 14° ,

$$\Delta\Omega = 35 \text{ msr},$$

Spin precession angle is $\sim 90^\circ$
(it is optimum)

Event rate is **15 times higher**
than with standard spectrometer

From 58 days of production time
resulting accuracy (for each of
two data points):

$$\Delta(\mu G_E^p / G_M^p) = \pm 0.10$$

SBS physics program - 2009

- **GEP** : reach unique high 15 (GeV/c)²
 - **GMN**: reach absolute max 17 (GeV/c)²
 - **GEN**: reach fantastic value 10 (GeV/c)²
 - **SSA in nSIDIS**: 30,000 gain vs HERMES
-

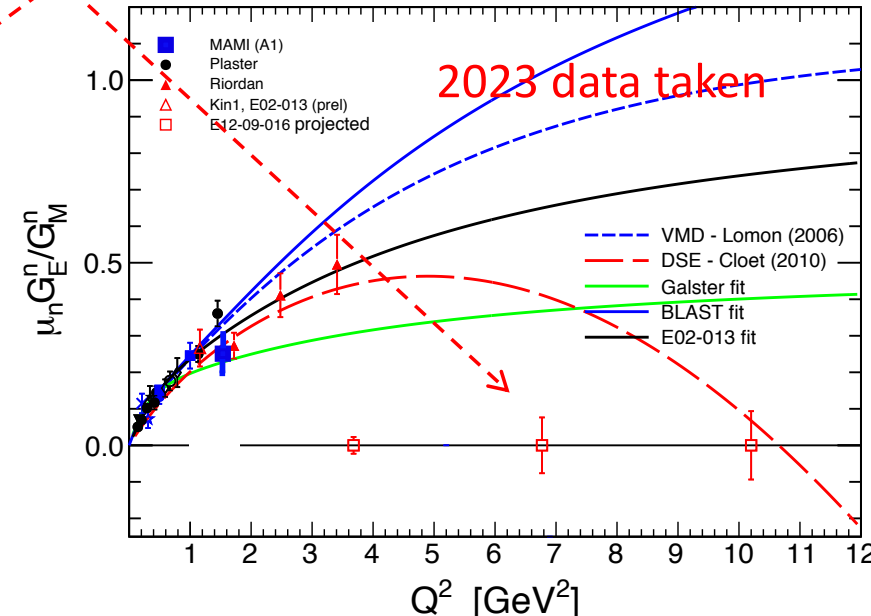
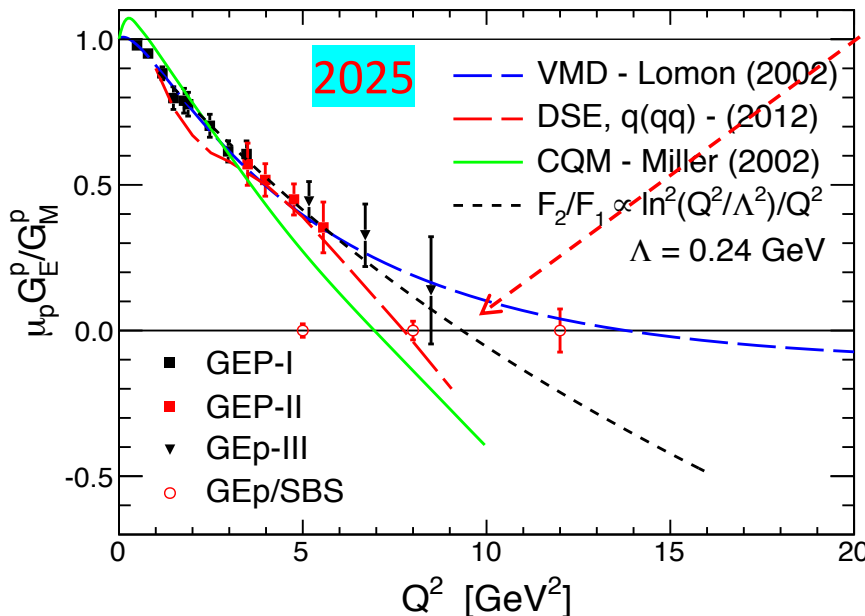
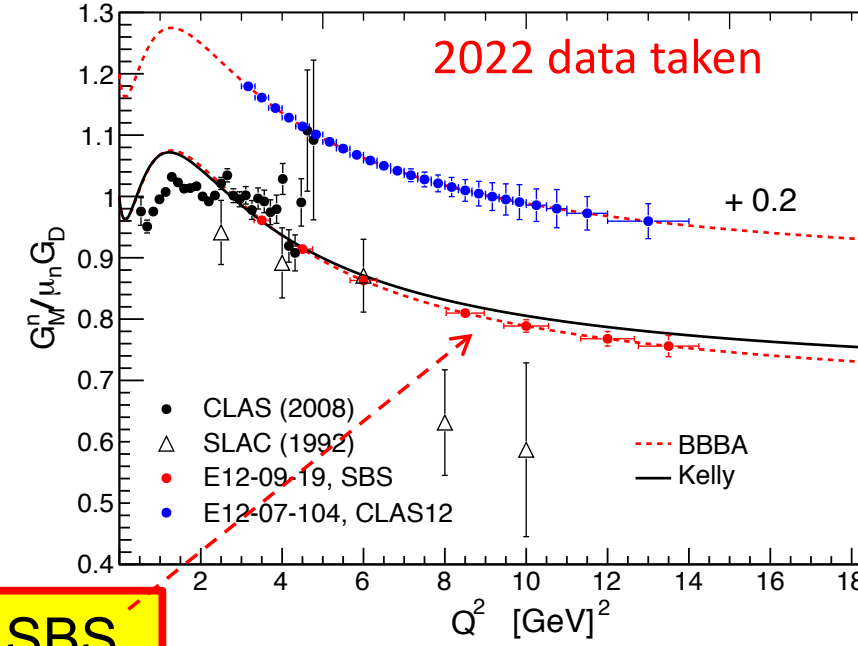
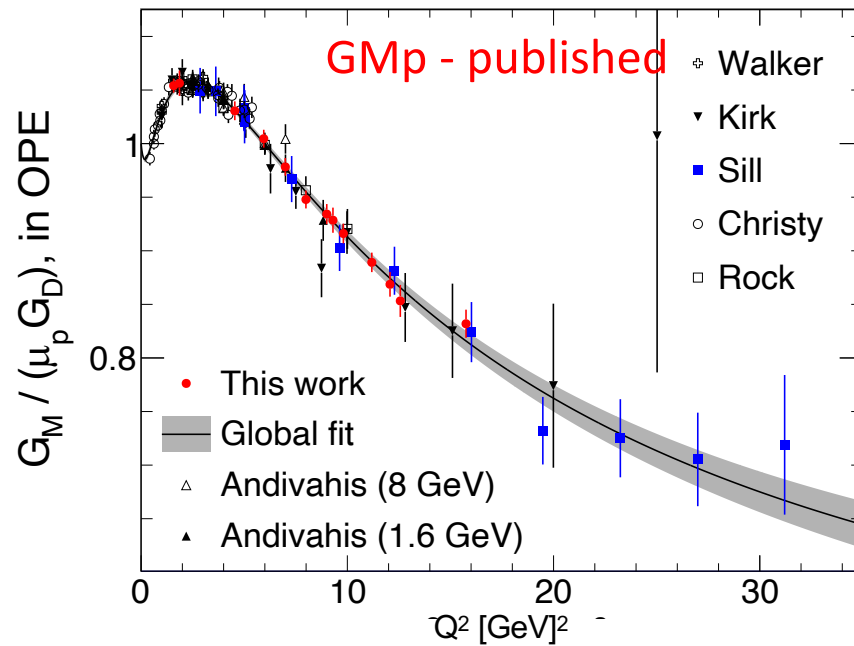
- D(e,e'p) – proton FFs ratio modification and Resonances
- **A1n/d2n** – gain ~ 20-30 compared with HMS/SHMS
- A1p/d2p – same
- D(e,e'd) event rate gain ~ 50 at 6 (GeV/c)²
- T/³He(e,e') : 0.1 g of T in the target = 0.6% of Bates
- RCS. $d\sigma/dt, K_{LL}, A_{LL}$
- SRC: e'(HRS) + p(SBS) + N(BB)
- PVDIS – gain 10-15 compared with two HRS
- J/Psi as gluon probe of QCD – well matched to SBS
- J/Psi production – gain 50 compared with SHMS+HMS
- A(e,e'p), A(e,e' π^{+-}), A(e,e' ϕ) - each item - big program

SBS physics program - 2024

- GMn – up to 13.5 GeV²
- L/T cross section for neutron - nTPE
- GEn (He-3) – up to 10 GeV²
- GEn-RP ($n \rightarrow p$ & $n \rightarrow n$ polarimeters)
- Wide Angle Pion Production => KLL
- ~~WAPP from polarized He-3: --> ALICE~~ (beam dump failed)
- GE_p ($p \rightarrow p$ polarimeter) – up to 12 GeV²

- SIDIS - approved
- TDIS - cond. approved
- Pol WACS. - approved; CPS => $L_{\gamma p} = 5 \times 10^{35}$, FM gain 100
- Strange FF at 2.5 GeV² - approved
- Axial FF at 1 GeV² - LOI12-24-009
- SBS + CPS + NH3/ND3 for $D(\gamma, \pi+n)$, $D(\gamma, p+n)$, $H(\gamma, \pi+N)$
- GMn at 15.5 and 18 GeV²
- GEn-RP at 7-8 GeV²
- g1, g2 for DIS with 12 GeV and BB/SBS
- DVCS on transversely polarized target with SBS+NPS
- ϕ as Deeply Virtual Vector Meson production

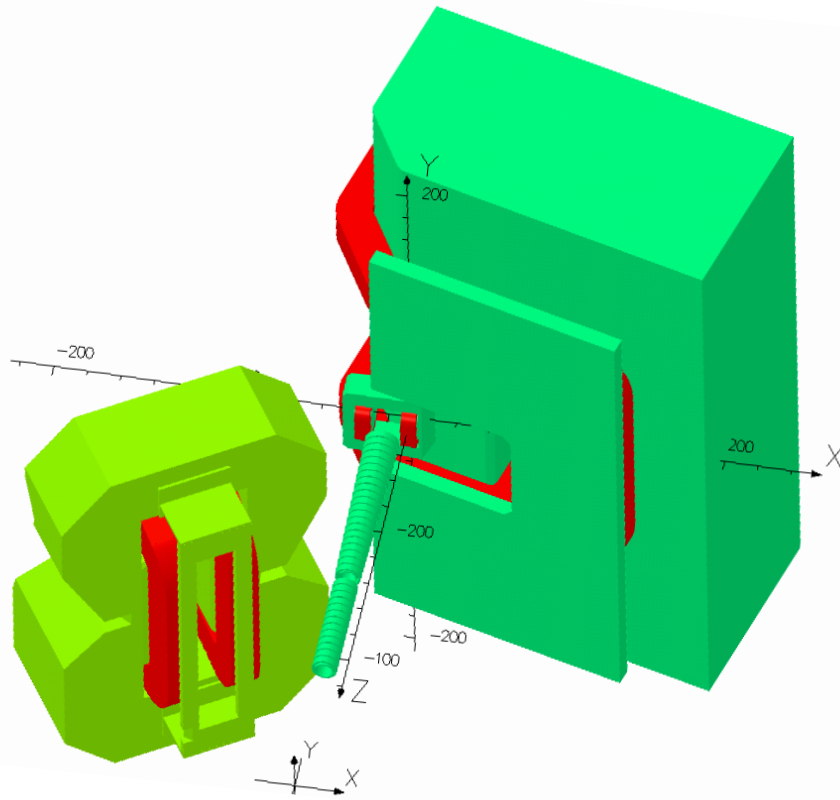
The nucleon FFs



Where is SBS/BB useful?

- High Q^2 , e.g. elastic Form Factors, DVCS
- Large acceptance, e.g. polarized target
- Two-arm high- z experiments, e.g. SIDIS

Two-arm SBS/BB setup



$$\sigma_p/p = 0.08 + 0.004 \times p[\text{GeV}]$$

$$\sigma_\theta = 1 - 2, \text{ mrad}$$

$$\Omega = 70 - 90 \text{ msr, for } \theta \geq 30^\circ$$

$$\sigma_p/p = 0.0029 + 0.0003 \times p[\text{GeV}]$$

$$\sigma_\theta = 0.14 + 1.3/p[\text{GeV}], \text{ mrad}$$

$$\Omega = 72 \text{ msr, for } \theta \geq 15^\circ$$

$$\Omega = 30 \text{ msr, for } \theta = 7.5^\circ$$

One- and Two-Arm experiments (O&TA)

Many productive experiments in the field belong to
the category One- and Two-Arm:

Among them are DIS, SIDIS, FFs (GEP), WACS, DVCS,

The main advantage of these “simple” (e,e') and ($e,e'h/g$) is
the simplicity of such processes for physics interpretation

The productivity of an experiment or Figure-of-Merit:

$$FOM = \mathcal{L} \times \Omega_1 (\times \Omega_2)$$

One- and Two-Arm experiments (O&TA)

$$FOM = \mathcal{L} \times \Omega_{electron} = 10^{38} \cdot 0.07 = 7 \times 10^{36}$$

electron/s × nucleon/cm² × sr

Now we can formulate detector configuration
for productive one- and two-arm experiments

- Magnetic analysis with “vertical bend”
- Moderate solid angle
- Independent arms
- Small angle capability
- Space for segmented PID, polarimeter

One- and Two-Arm experiments (O&TA)

$$FOM = \mathcal{L} \times \Omega_{electron} = 10^{38} \cdot 0.07 = 7 \times 10^{36}$$

electron/s × nucleon/cm² × sr

Now we can formulate detector configuration
for productive one- and two-arm experiments

- Magnetic analysis with “vertical bend” => protected detector
- Moderate solid angle => high luminosity
- Independent arms => full range of angles
- Small angle capability => high x, t, low x
- Space for segmented PID, polarimeter => RICH counter, HCAL

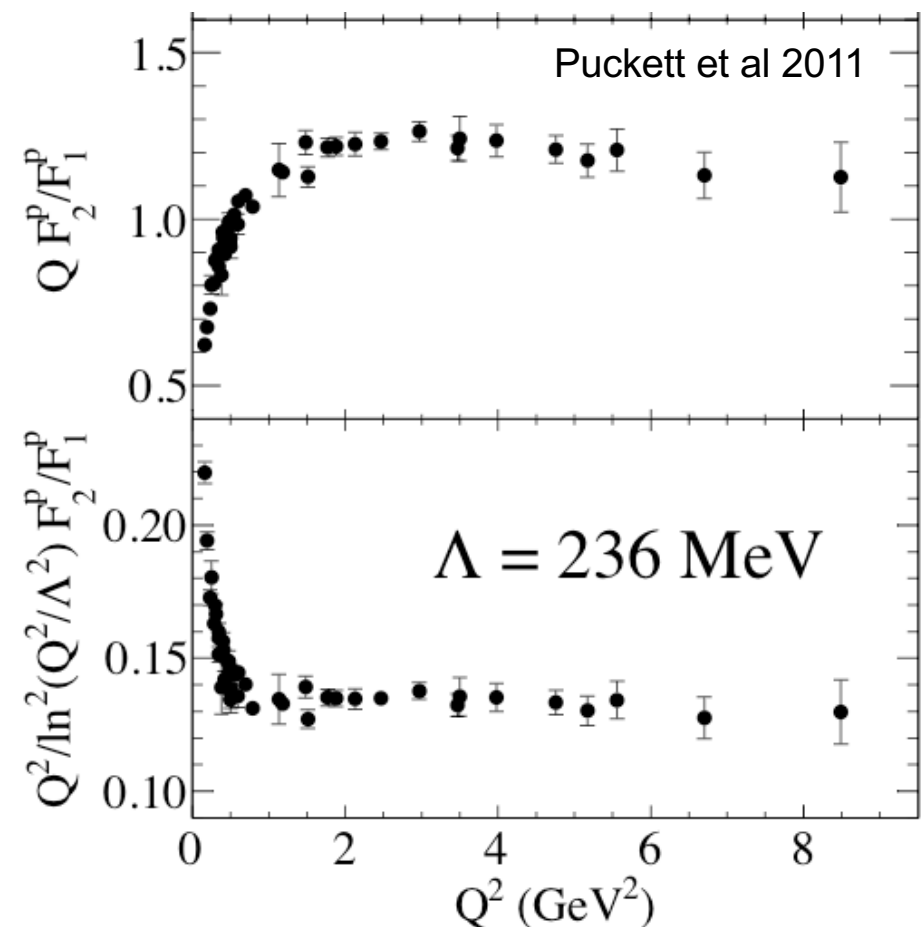
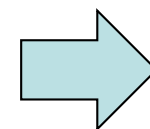
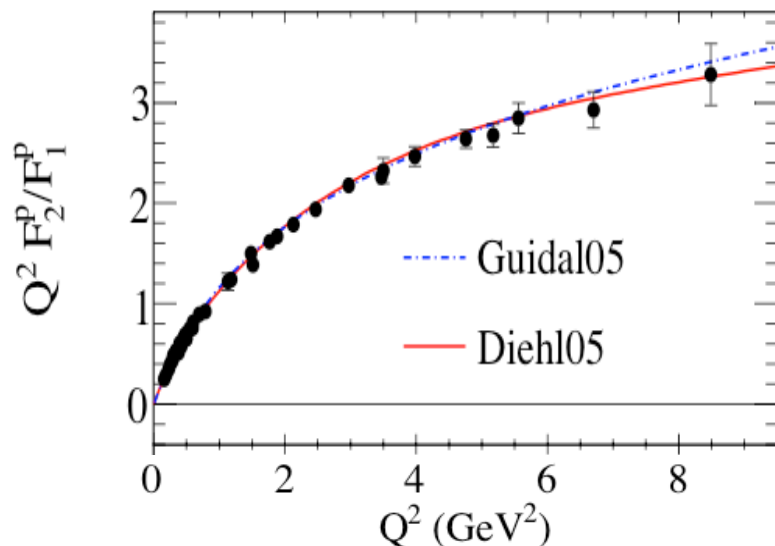
The goal is understanding of the nucleon

From the Sachs FFs to the ratio F_2/F_1
and the Belitsky, Ji, Yuan “log” scaling

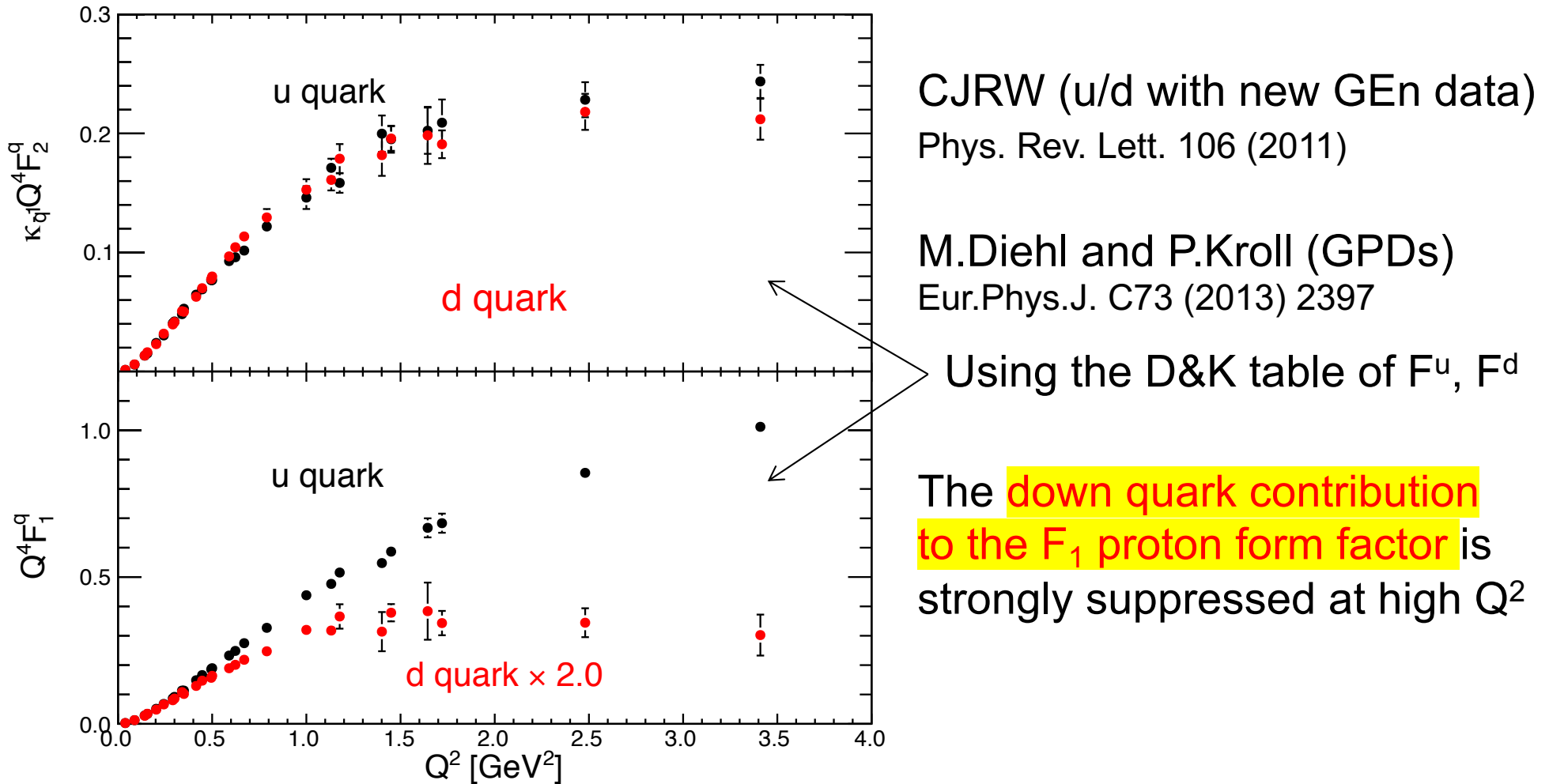
Orbital moment !

$$F_1 = \frac{G_E + \tau G_M}{1+\tau} \quad F_2 = -\frac{G_E - G_M}{1+\tau}$$
$$\tau = Q^2/4M^2$$

$$Q^2 F_2/F_1 \propto \frac{1-G_E/G_M}{1 + [G_E/G_M]/\tau}$$

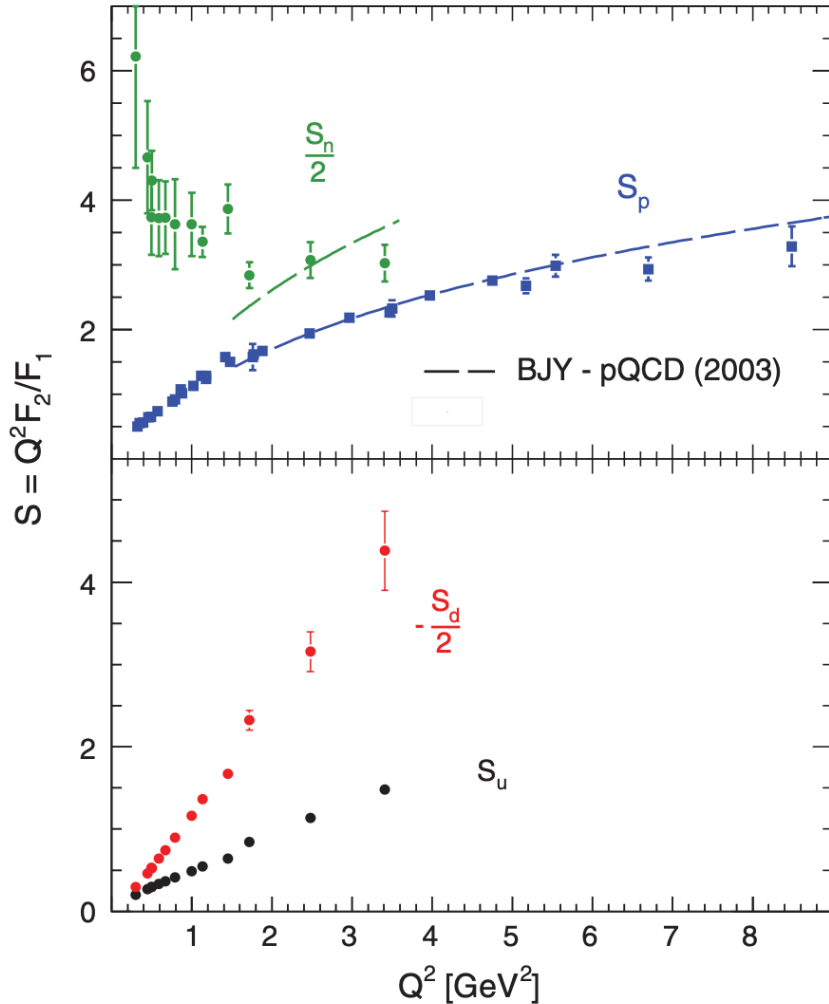


Flavor contributions to the nucleon FFs



Experimental Program

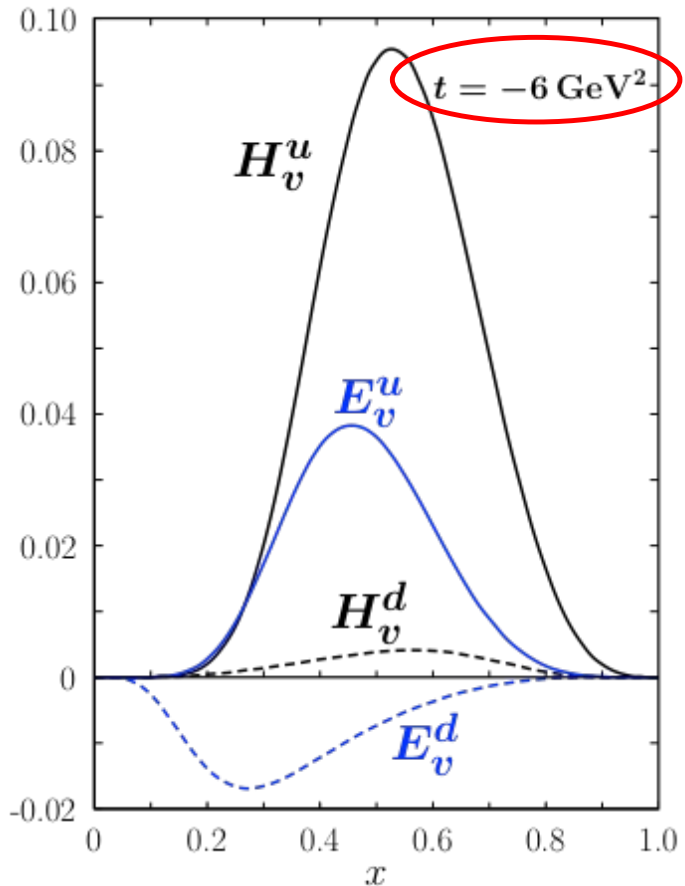
Flavor contributions to the nucleon FFs



The Q^2 range < 3.4 GeV 2 is too early for BJY scaling and orbital moment impact

There is a large effect from the reduction of F_1^d

Diehl-Kroll GPDs analysis (2013)



$$F_1(t) = \sum_q e_q \int dx H_q(x, t)$$

$$q(x, b) = \int \frac{d^2 q}{(2\pi)^2} e^{i \mathbf{q} \cdot \mathbf{b}} H_q(x, t = -\mathbf{q}^2)$$

$$\rho(b) \equiv \sum_q e_q \int dx q(x, b) = \int d^2 q F_1(\mathbf{q}^2) e^{i \mathbf{q} \cdot \mathbf{b}}$$

$$\rho(b) = \int_0^\infty \frac{Q \cdot dQ}{2\pi} J_0(Qb) \frac{G_E(Q^2) + \tau G_M(Q^2)}{1 + \tau}$$

center of momentum $\mathbf{R}_\perp = \sum_i x_i \cdot \mathbf{r}_{\perp,i}$

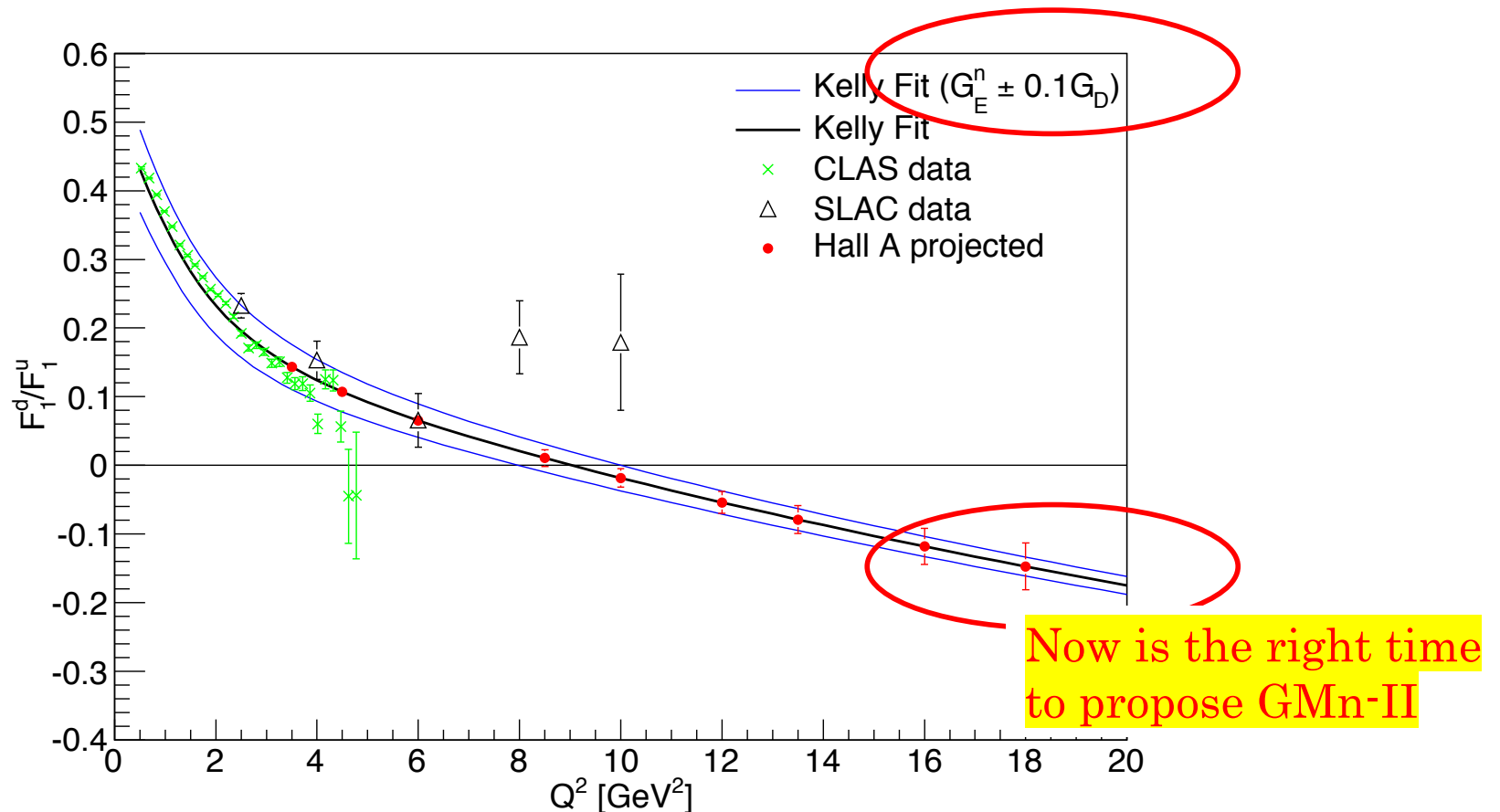
\mathbf{b} is defined relative to \mathbf{R}_\perp

At $t = -6 \text{ GeV}^2$ H^d is 12 times smaller H^u

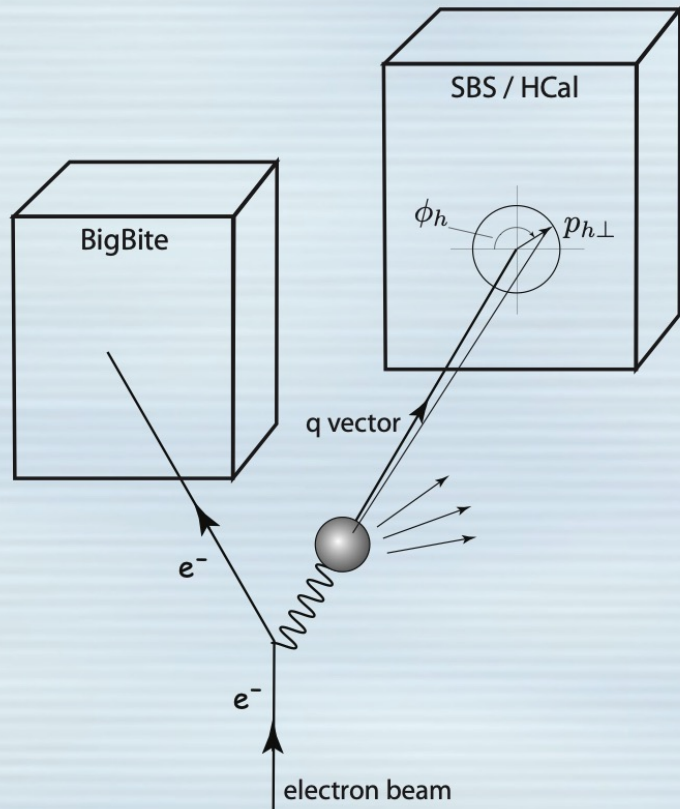
Positive $H^d \Rightarrow$ negative F_1^d

F_1 decomposition at very large Q^2

$$F_1 = \frac{G_E + \tau G_M}{1 + \tau} \quad F_2 = -\frac{G_E - G_M}{1 + \tau}$$



The concept behind the SBS SIDIS experiment



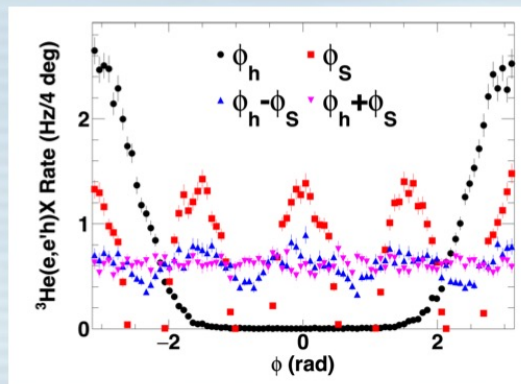
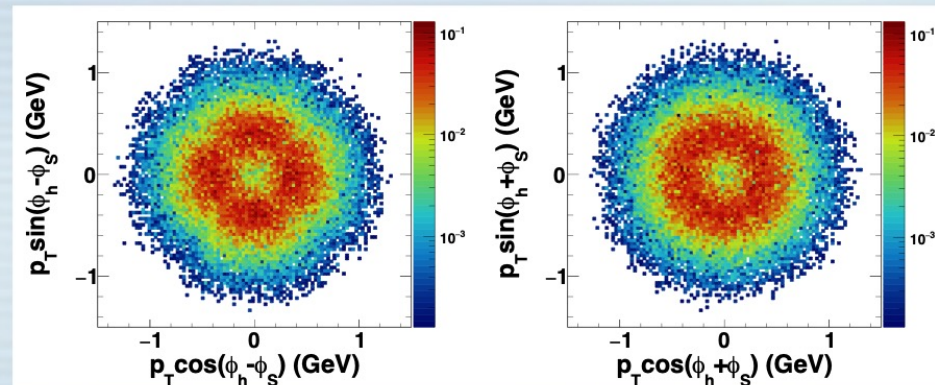
- The open-geometry dipole spectrometers allow wide kinematic coverage with a single setting.
- GEM-based tracking can handle huge singles rates.
- Center the hadron arm on q
- Exploit kinematic focusing along q
- Polarized ${}^3\text{He}$ target has flexibility to orient polarization relatively freely in the plane perpendicular to q .

By judicious positioning of the hadron arm, even moderate solid angle results in excellent statistics.

Slide from G. Cates & A. Puckett

SIDIS, E12-09-018

SBS SIDIS Azimuthal Coverage

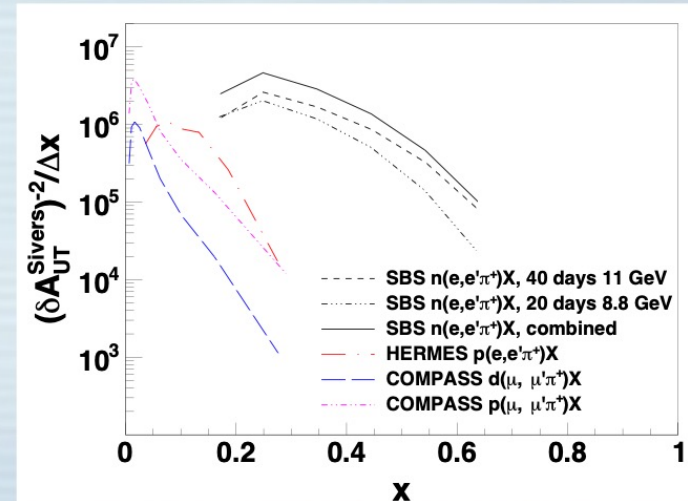
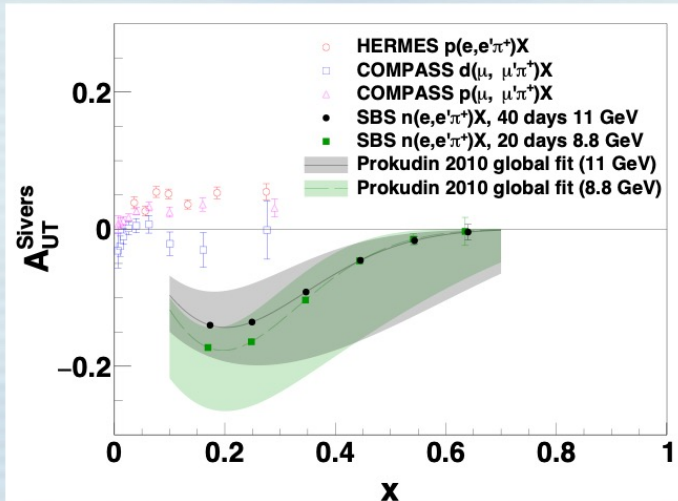


- Our original proposal envisioned eight spin orientations.
- We find virtually unchanged azimuthal coverage (and overall FoM) with four.
- Limiting to four spin orientations greatly simplifies the polarized target, enabling the use of major portions of the G_E^n target.

Slide from G. Cates & A. Puckett

SIDIS, E12-09-018

Comparing SBS SIDIS neutron data with existing data



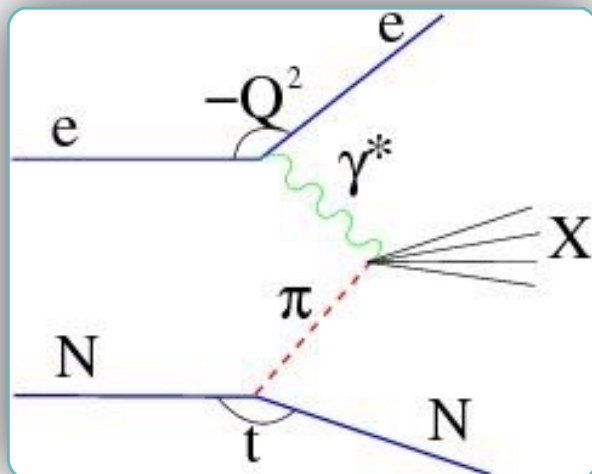
- SBS SIDIS will increase the statistics of available TMD data by a factor of ~ 100 !!!
- At higher values of x , roughly $x > 0.1$, it will completely dominate TMD measurements for many years to come.

Slide from G. Cates & A. Puckett

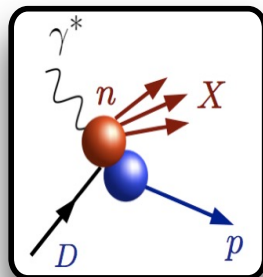
Tagged DIS, C12-14-010

will use spectator tagging - a well established technique-
to tag the “meson cloud” of the nucleon.

The Sullivan process

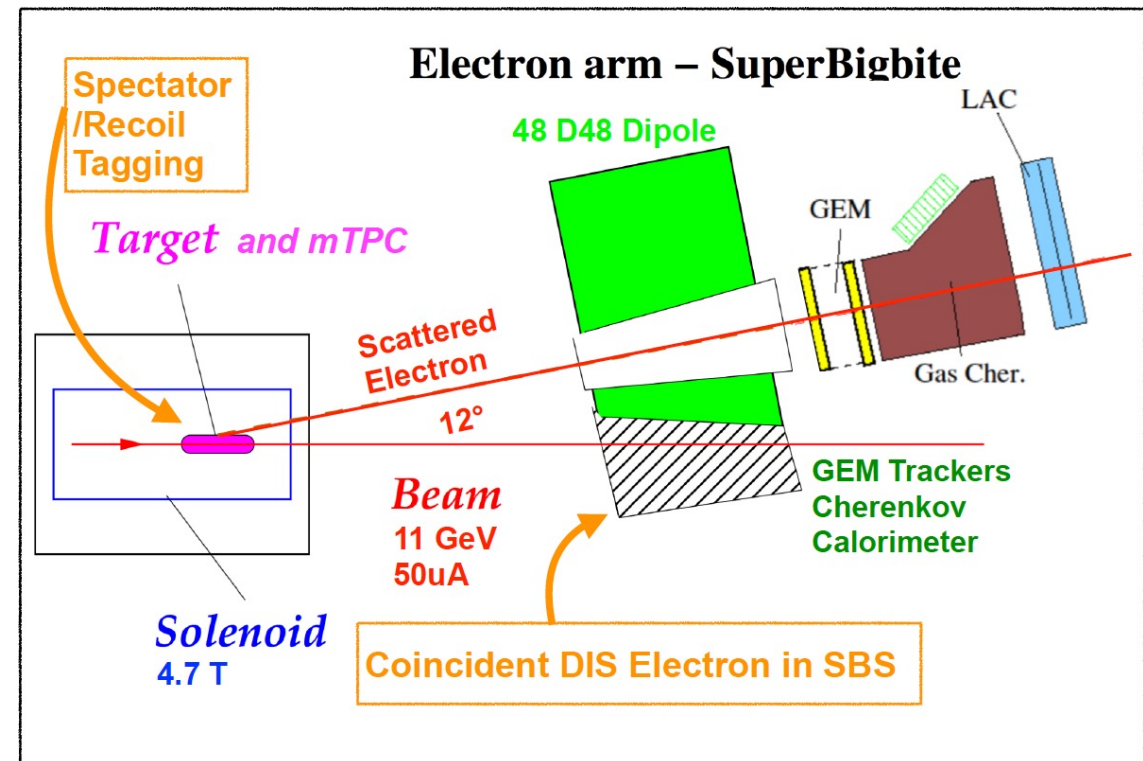


almost free neutron



Deuteron Spectator proton

(backward going slow proton)

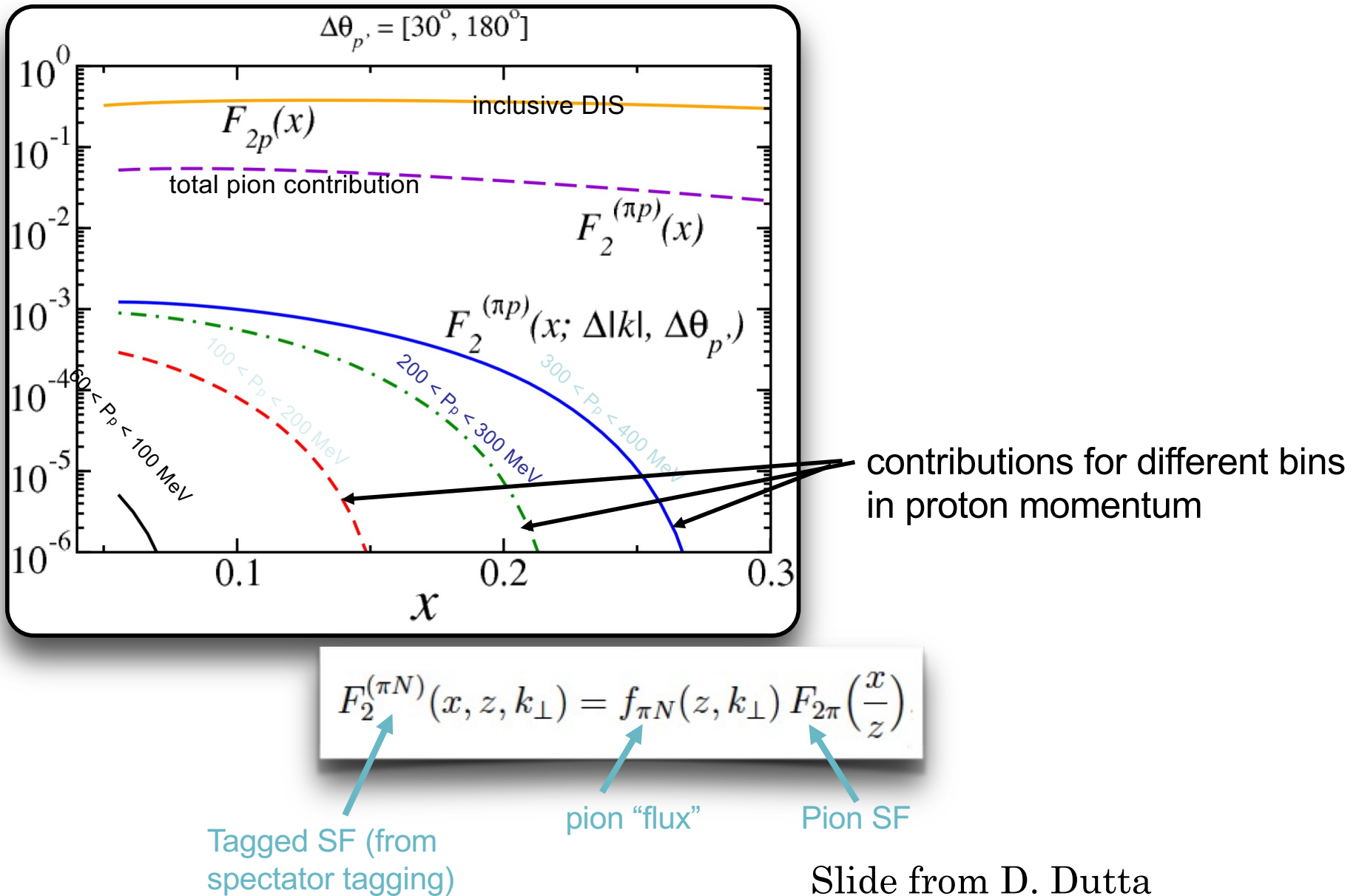


TDIS is a pioneering experiment that will provide the first direct measure of the mesonic content of nucleons.

The technique used to extract meson structure function is a necessary first step for future experiments at the EIC & 22 GeV JLab.

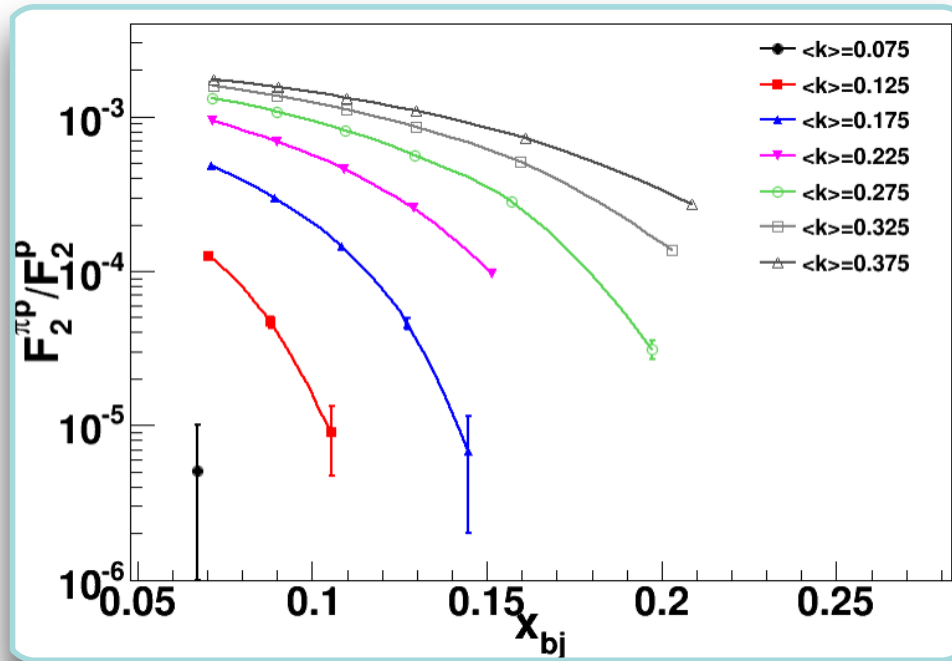
Slide from D. Dutta

Tagged structure functions to pion structure function

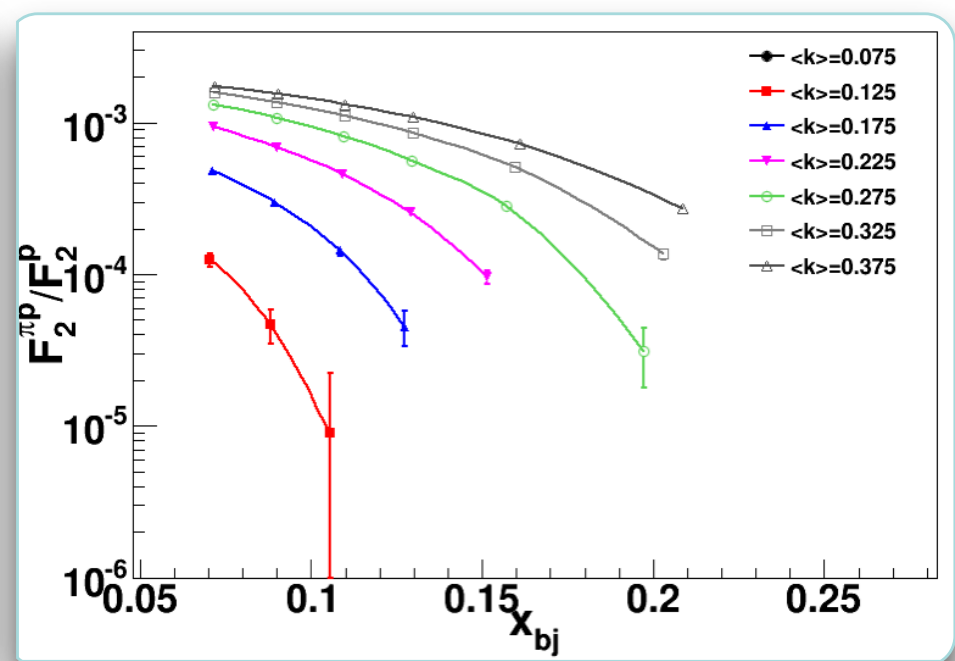


The TDIS experiment will measure tagged structure functions for protons and neutrons

proton target



neutron target



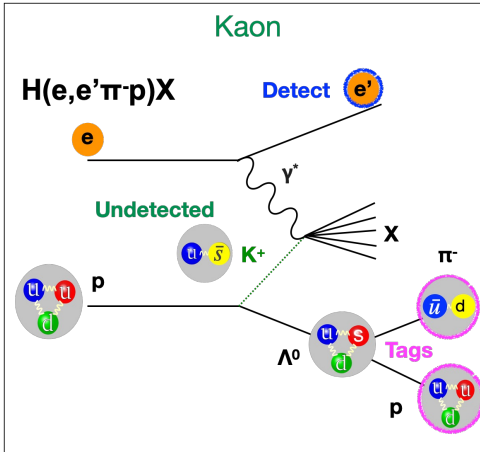
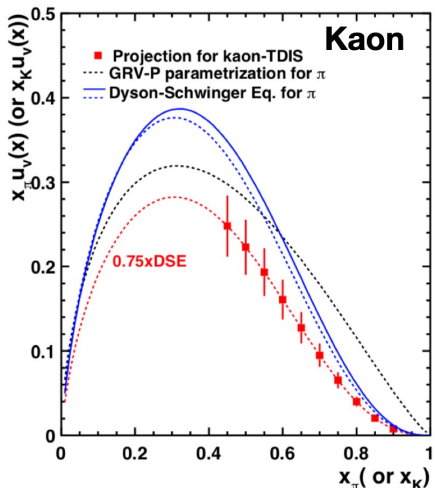
Full momentum range (collected simultaneously) - all momentum bins in MeV/c
 Error bars largest at highest x points - at fixed x, these are the lowest t values

some kinematic limits:

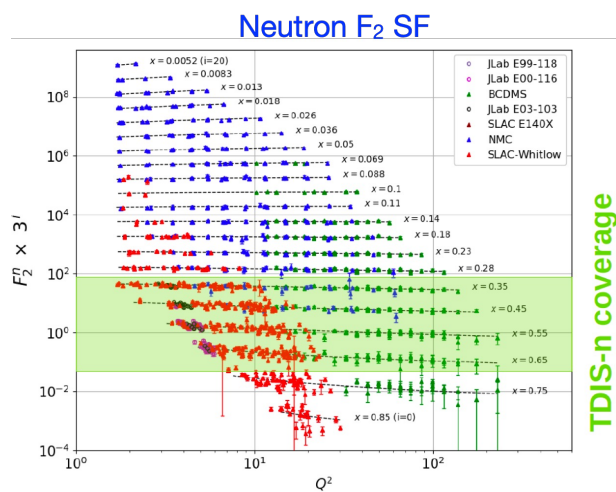
- $150 < k < 400$ MeV/c corresponds to $z < \sim 0.2$
- Also, $x < z$
- Low x, high W at 11 GeV means $Q^2 \sim 2$ GeV 2

Slide from D. Dutta

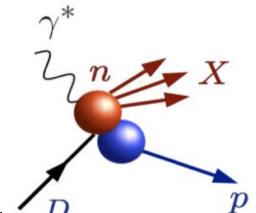
Approved TDIS run Groups



- Kaon TDIS - Run group C12-15-006A PAC45
- No additional beam time/detectors
- First Sullivan process extraction of kaon SF
- Comparing pion and kaon structure will be a key tool to study emergent hadronic mass



- TDISn - Run Group C12-15-006B PAC49
- Use deuterium as effective free neutron target
- Neutron SF... plus resonance region SF, EMC effect in deuteron, elastic e-n scattering and EM form factor G_M^n
- c.f. BoNuS, BoNuS12, MARATHON
- Independent cross-check of systematics
- Increased statistics in TDISn range
- Calibrate mTPC acceptance and efficiency
- QE scattering on deuteron: HCAL for n; mTPC for p; SBS for e
- Independent normalisation check of tagging method across experiments



Slide from R. Montgomery

Experiments on the polarized solid target

- Polarized Wide Angle Compton Scattering, E12-17-008
- Pion photoproduction from neutron – replacement of ALL/He-3
- Polarized deuteron to p-n – higher photon energy
- Pion photoproduction from proton
- T20 in D($e,e'd$) – 10-20x larger solid angle
- Proton g1/g2 – 10-20x larger solid angle

Polarized WACS, E12-17-008

D. Day, D. Hamilton, D. Keller, G. Niculescu, B. Wojtsekhowski and J. Zhang

- ① A $2.5 \mu\text{A}$ polarized electron beam incident on a 10 % radiator inside a new Compact Photon Source (CPS) produces a high-intensity untagged photon beam.
- ② The proton target is the UVA/JLab solid polarized ammonia target.
- ③ The recoil proton is detected with the BigBite spectrometer equipped with GEM trackers and trigger detectors.
- ④ The highly-segmented PbWO_4 NPS calorimeter is used to detect the scattered photon.

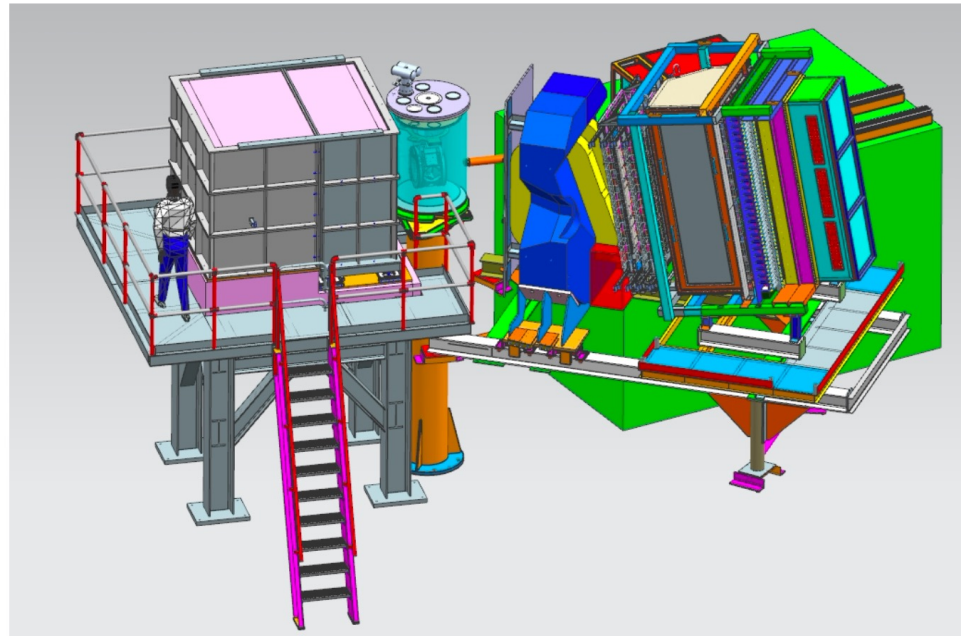


Figure from Steve Lassiter

The use of the CPS and BigBite results in a factor of 30 improvement in figure-of-merit over previous experiments and opens up a new range of polarized physics opportunities at JLab.

Slide from D. Hamilton

Polarized WACS, CPS

A conceptual design study of a Compact Photon Source (CPS) for Jefferson Lab [NIM-A 957 \(2020\) 163429](#)

D. Day ^a, P. Degtiarenko ^b, S. Dobbs ^c, R. Ent ^b, D.J. Hamilton ^d, T. Horn ^{e,b,*}, D. Keller ^a, C. Keppel ^b, G. Niculescu ^f, P. Reid ^g, I. Strakovsky ^h, B. Wojtsekowski ^b, J. Zhang ^a

D. Day, P. Degtiarenko, S. Dobbs et al.

Nuclear Inst. and Methods in Physics Research, A 957 (2020) 163429

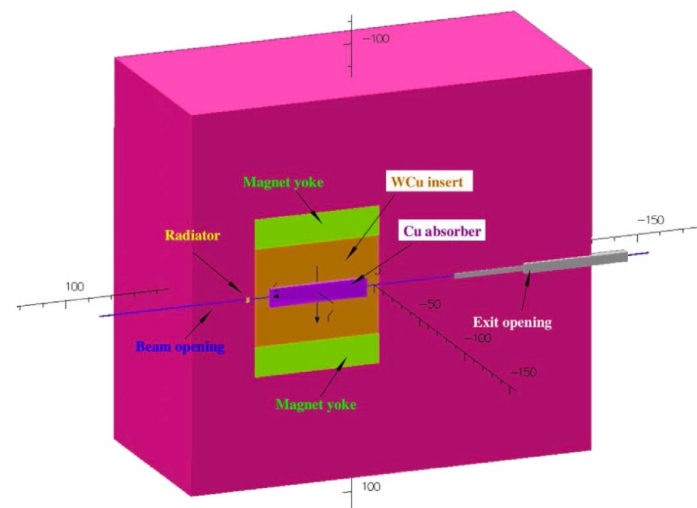


Fig. 3. The CPS cut-out side view. Deflected electrons strike a copper absorber, surrounded by a W-Cu insert inside the magnet yoke. The outer rectangular region in this view is the tungsten-powder shield.

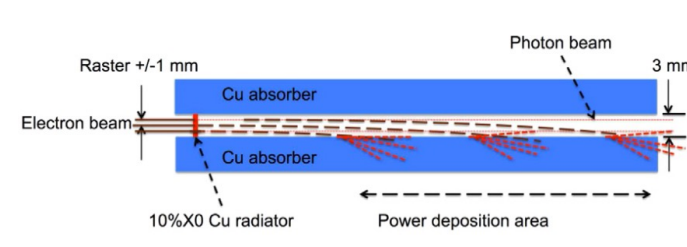


Fig. 4. The scheme of beam deflection in the magnetic field to the absorber/dump.

around the photon beam can be as narrow as the photon beam size. After passing through the radiator, the electron beam should be separated from the photon beam by means of deflection in a magnetic field. The length, aperture and field strength of the magnet are very different in the proposed source compared to in the traditional tagging technique. In the traditional source the magnet is needed to direct the electrons to the dump. Because of the large momentum spread of electrons which

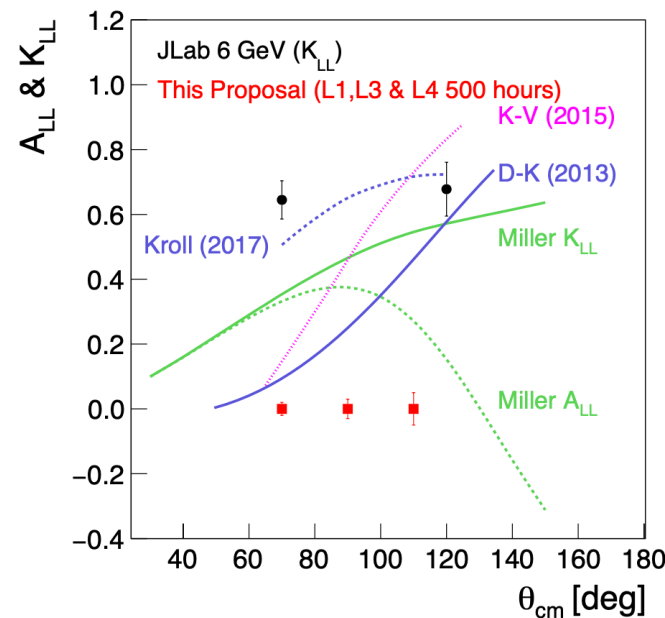
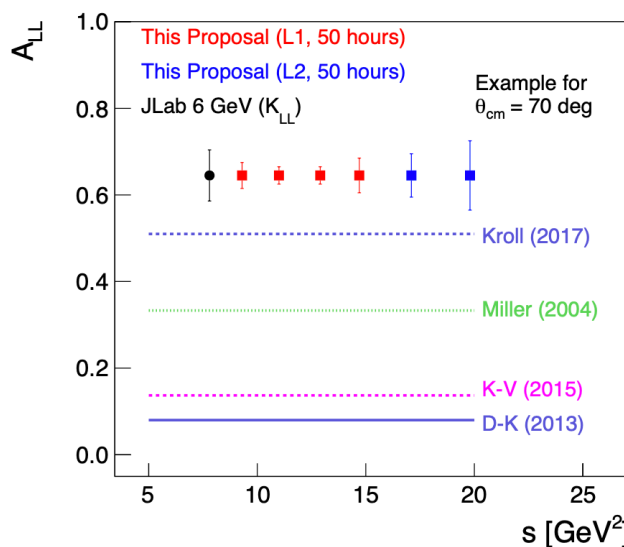
Polarized WACS, E12-17-008

$$\frac{d\sigma}{dt} = \left(\frac{d\sigma}{dt} \right)_{\text{KN}} \left\{ \frac{1}{2} \frac{(s-u)^2}{s^2 + u^2} \left[R_V^2(t) + \frac{-t}{4m^2} R_T^2(t) \right] + \frac{1}{2} \frac{t^2}{s^2 + u^2} R_A^2(t) \right\}$$

$$A_{LL} = K_{LL} = \frac{R_A(t)}{R_V(t)} A_{LL}^{\text{KN}}$$

Diehl & Kroll, EPJ C73 (2013)

$$A_{LS} = -K_{LS} = A_{LL} \left[\frac{\sqrt{-t}}{2m} \frac{R_T(t)}{R_V(t)} - \beta \right]$$

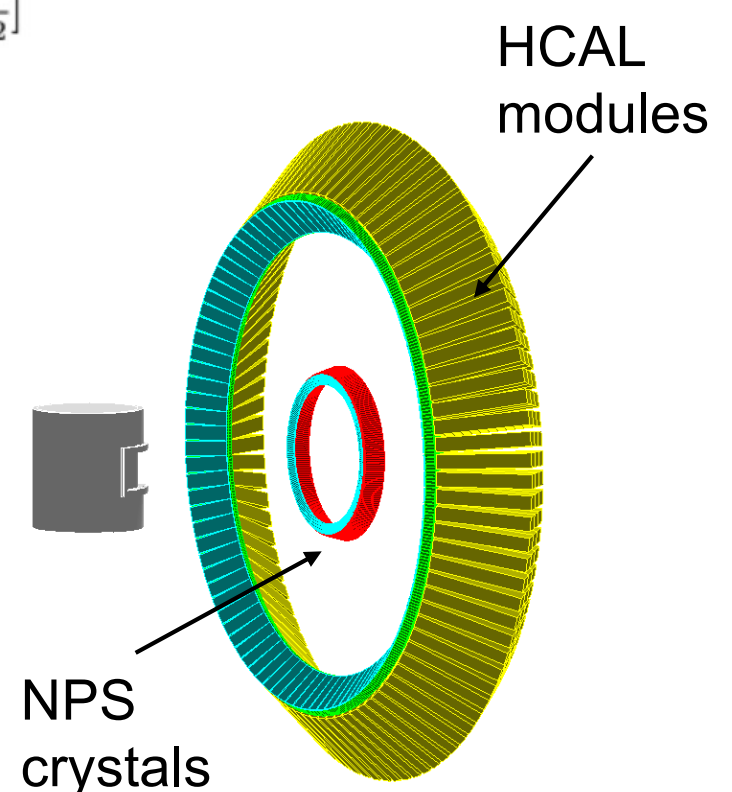
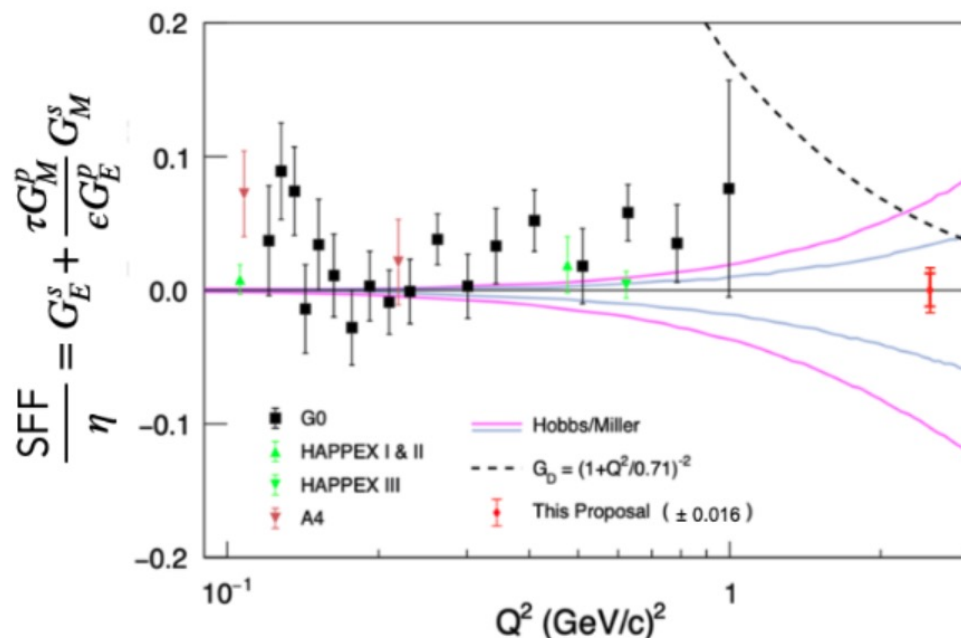


Slide from D. Hamilton

Nonzero Strange FF, E12-23-004

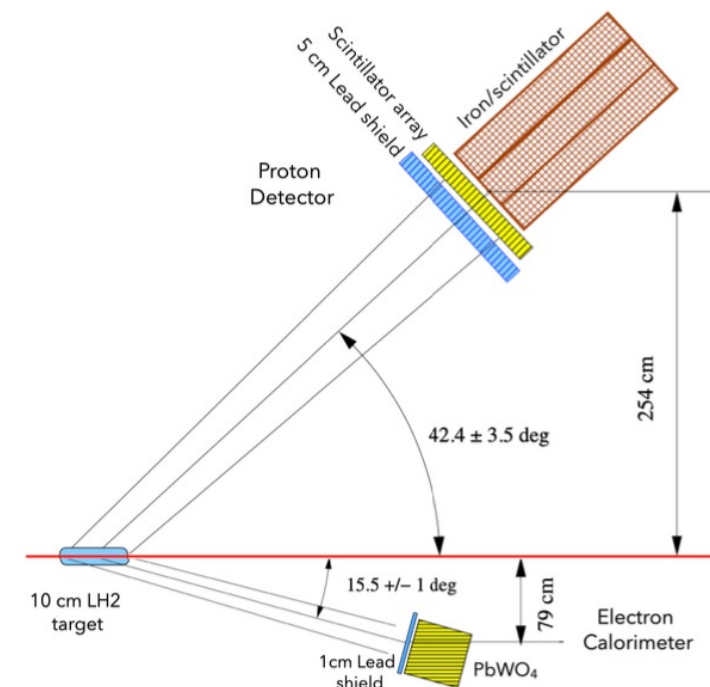
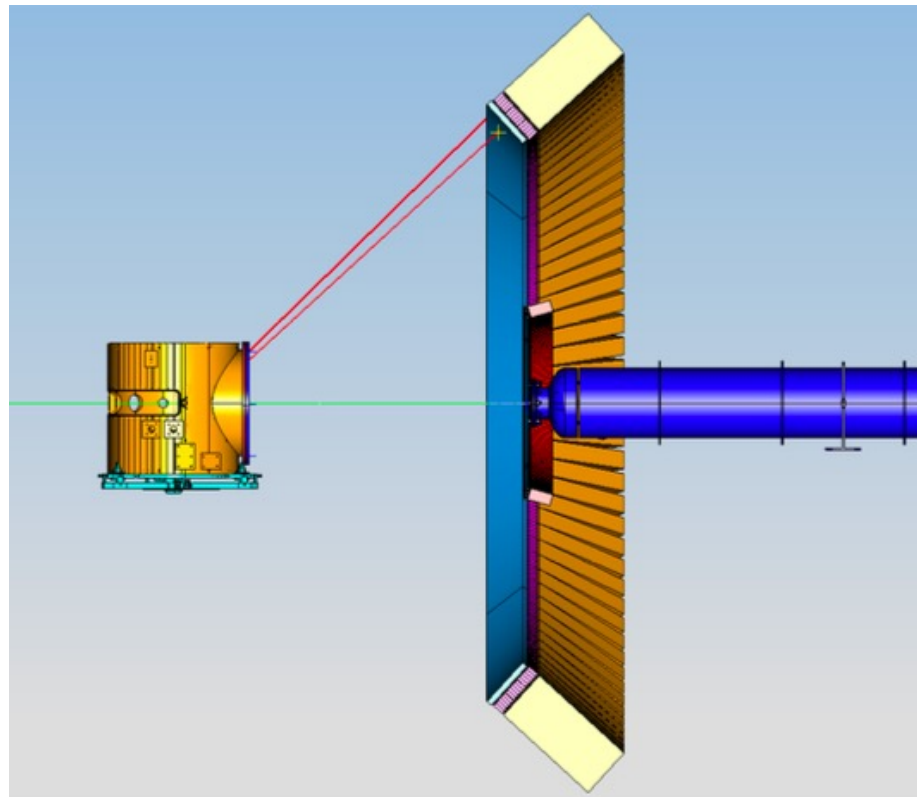
$$A_{PV} = -\frac{G_F Q^2}{4\pi\alpha\sqrt{2}} \cdot [(1 - 4\sin^2\theta_W) - \frac{\epsilon G_E^p G_E^n + \tau G_M^p G_M^n}{\epsilon(G_E^p)^2 + \tau(G_M^p)^2} - \frac{\epsilon G_E^p G_E^s + \tau G_M^p G_M^s}{\epsilon(G_E^p)^2 + \tau(G_M^p)^2}]$$

$$+ \epsilon'(1 - 4\sin^2\theta_W) \frac{G_M^p G_A^{Zp}}{\epsilon(G_E^p)^2 + \tau(G_M^p)^2}]$$



Slide from K. Paschke

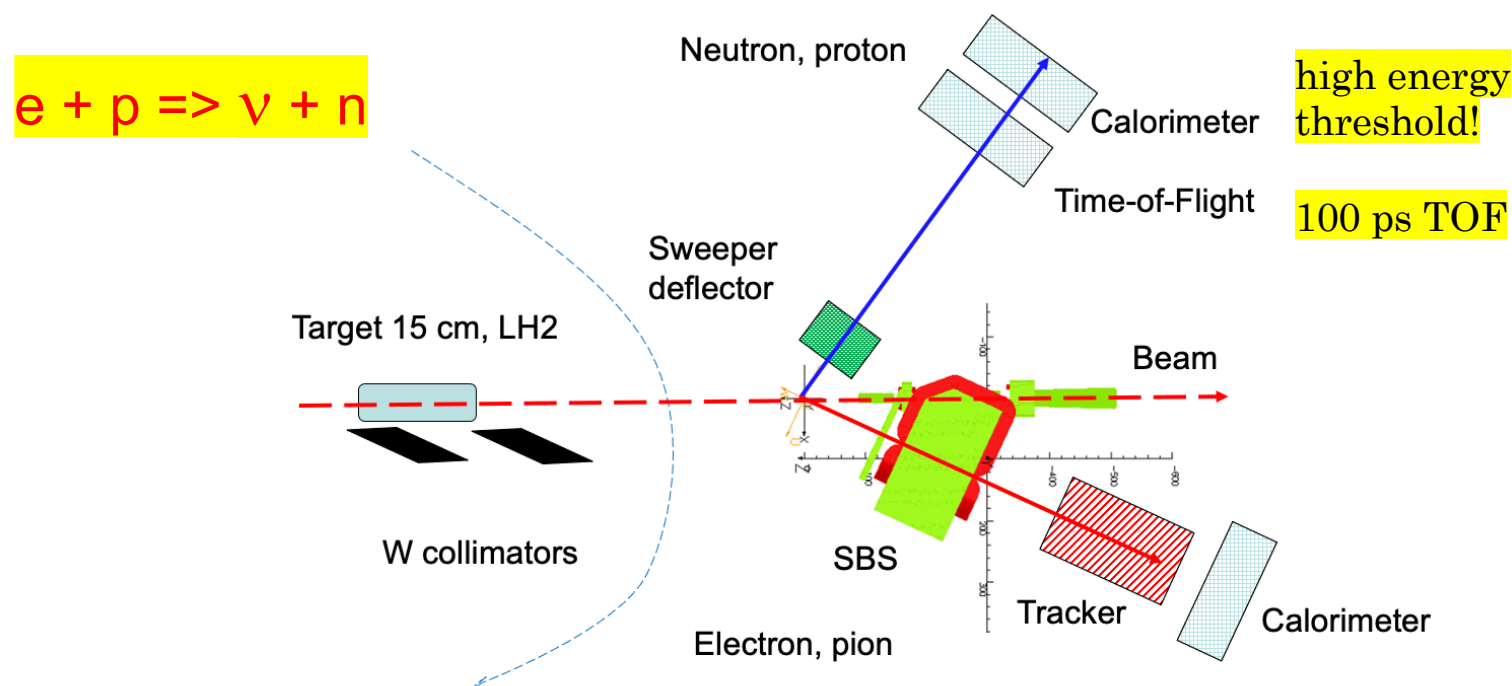
Nonzero Strange FF, E12-23-004



Slide from K. Paschke

Axial-vector Form Factor, LOI12-24-009

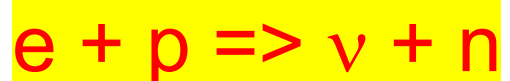
J. Napolitano, B. Wojtsekhowski, and
P. Degtiarenko, A. Deur, J. Golak, D. Jones,
C. Keppel, D.E. King, E. Cisbani, R. Perrino, O. Benhar,
D. Armstrong, T. Averett, M. Bukhari



Challenges in the study of $e + p \rightarrow \nu + n$ process

- Cross section for the weak process is $\sim 10^{-39} \text{ cm}^2/\text{sr}$
- Pion photo-production cross section $\sim 10^8$ of the weak one
- Proton rate from electron elastic e-p $\sim 10^7$ of the weak one

Axial-vector Form Factor, LOI12-24-009



Rejection of e-p and π -n events allows to increase S/B to 1/1000

After that measurement of helicity asymmetry allows to get result

The detectors are SBS spectrometer for a electron/pion arm and a neutron arm with a TOF (100 ps) and a hadron calorimeter

Neglecting pion events for brevity:

$$N_{\nu-n} = N_{total} - N_{e-p} = N_{total} \times [A_{observed} - 0.05 \times 10^{-3}]$$

$$\left[1 \times N_{\nu-n} + 0.5 \times 10^{-4} \times N_{e-p} \right] / N_{total} \sim N_{\nu-n} / N_{e-p} \sim 1/1000$$

$$1 \times 10^{-3} + 0.05 \times 10^{-3}$$

Double polarized $H(\gamma, \pi + p)$

SBS allows
FM gain 20+

K. WIJESOORIYA *et al.*

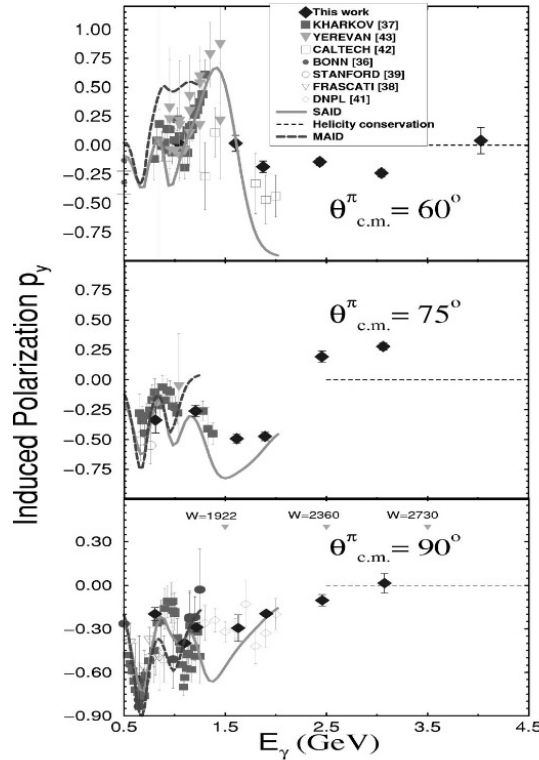


FIG. 9. Top to bottom: Induced polarization p_y in neutral pion photo-production at $\theta_{c.m.} = 60^\circ$, 75° , and 90° . Only statistical uncertainties are shown. The three curves, SAID [22], MAID [23], and helicity conservation shown in the figures are described in the text. Corresponding W range is also shown in the bottom plot.

PHYSICAL REVIEW C 66, 034614 (2002)

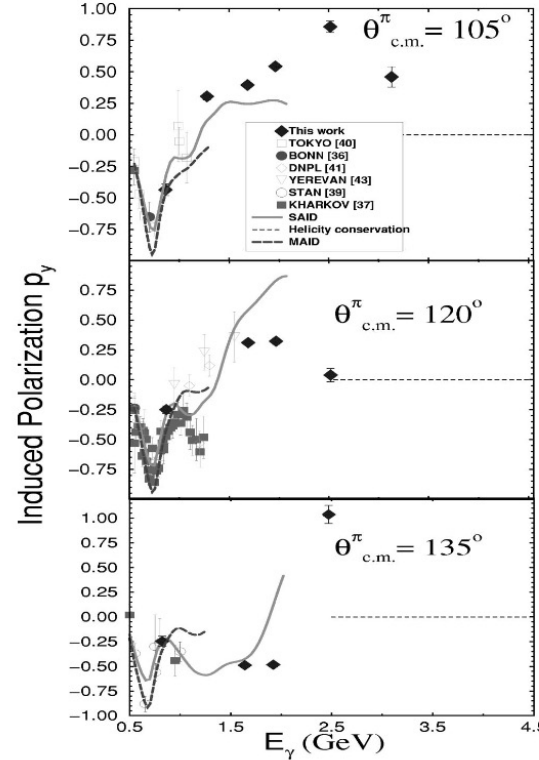


FIG. 10. Top to bottom: Induced polarization p_y in neutral pion photo-production at $\theta_{c.m.} = 105^\circ$, 120° , 135° . Only statistical uncertainties are shown. The three curves SAID [22], MAID [23], and helicity conservation shown here are described in the text.

Double polarized D(γ , p + n)

VOLUME 86, NUMBER 14

PHYSICAL REVIEW LETTERS

SBS allows
FM gain 20+

2 Apr

Polarization Measurements in High-Energy Deuteron Photodisintegration

K. Wijesooriya,^{10,*} A. Afanasev,^{20,26} M. Amarian,¹¹ K. Aniol,³ S. Becher,⁹ K. Benslama,²³ L. Bimbot,²² P. Bosted,¹⁶

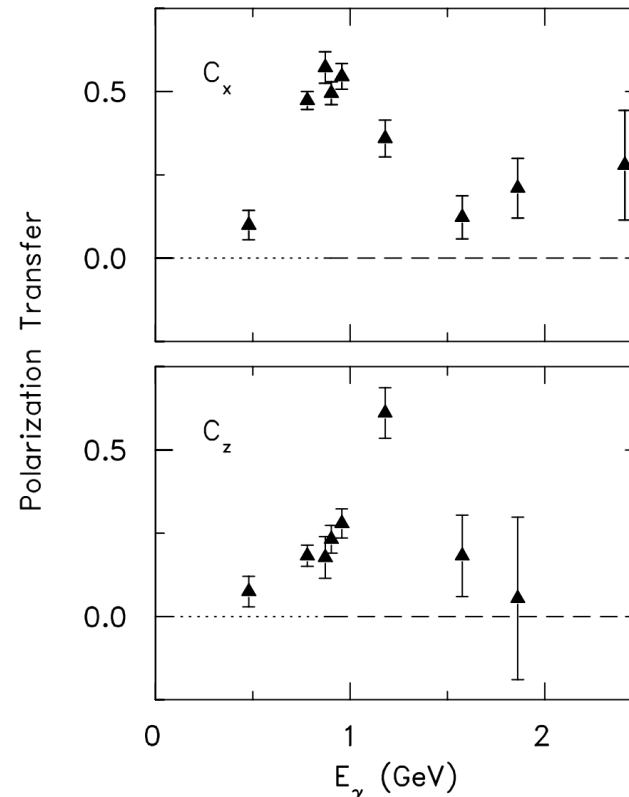


FIG. 2. Polarization transfers C_x and C_z in deuteron photodisintegration at $\theta_{\text{c.m.}} = 90^\circ$. Only statistical uncertainties are shown.

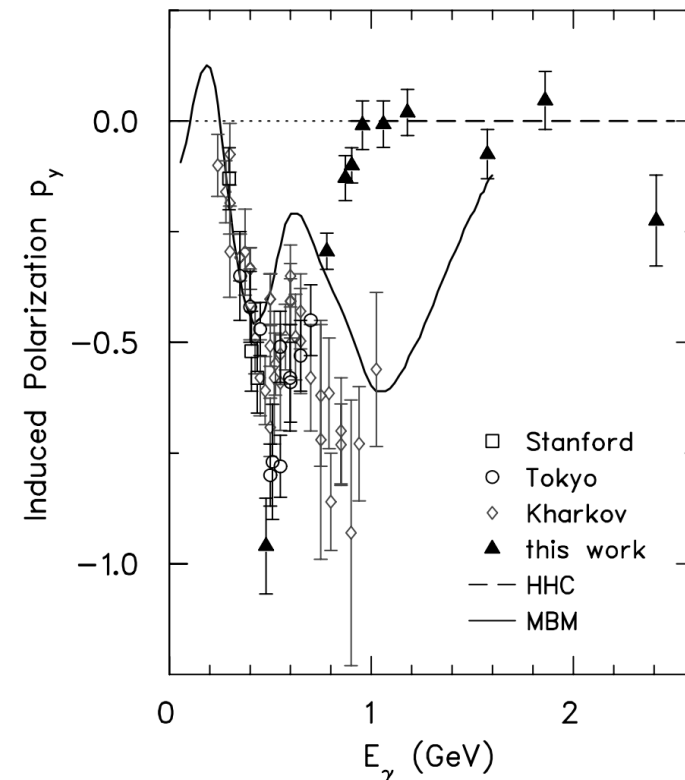


FIG. 1. Induced polarization p_y in deuteron photodisintegration at $\theta_{\text{c.m.}} = 90^\circ$. Only statistical uncertainties are shown. The curves are described in the text.

High energy D(γ , p + n)

VOLUME 87, NUMBER 10

PHYSICAL REVIEW LETTERS

3 SEPTEMBER

SBS allows
FM gain 20+

Measurement of the High Energy Two-Body Deuteron Photodisintegration Differential Cross Section

E. C. Schulte,¹ A. Ahmidouch,² C. S. Armstrong,³ J. Arrington,⁴ R. Asaturyan,⁵ S. Avery,⁶ O. K. Baker,^{3,6}
D. H. Beck,¹ H. P. Blok,⁷ C. W. Bochna,¹ W. Boeglin,⁸ P. Y. Bosted,⁹ M. Bouwhuis,¹ H. Breuer,¹⁰ D. S. Brown,¹⁰

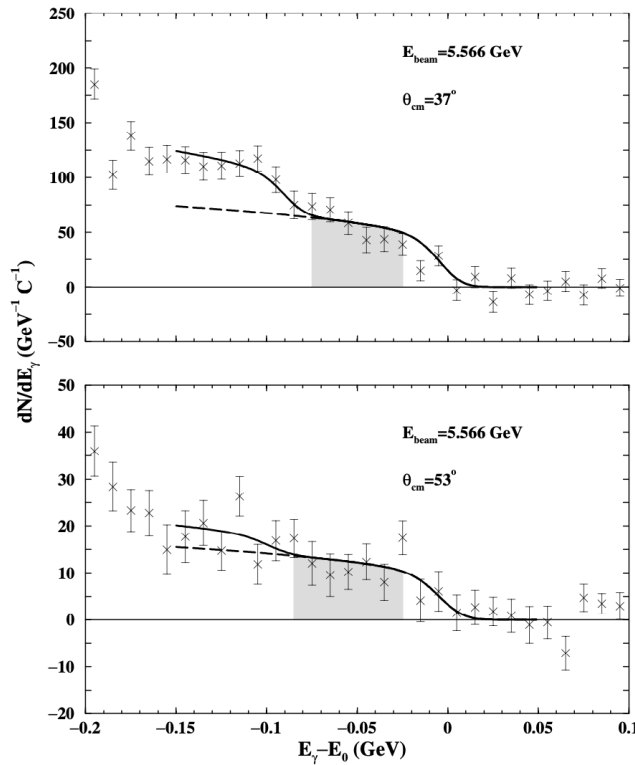


FIG. 1. Photon energy spectra, normalized to collected electron beam charge, for $\theta_{cm} = 37^\circ$ (top panel) and 53° (bottom panel) at 5.5 GeV. The grey shaded area denotes the region in E_γ where the photoproton yield is calculated. The curves are described in the text.

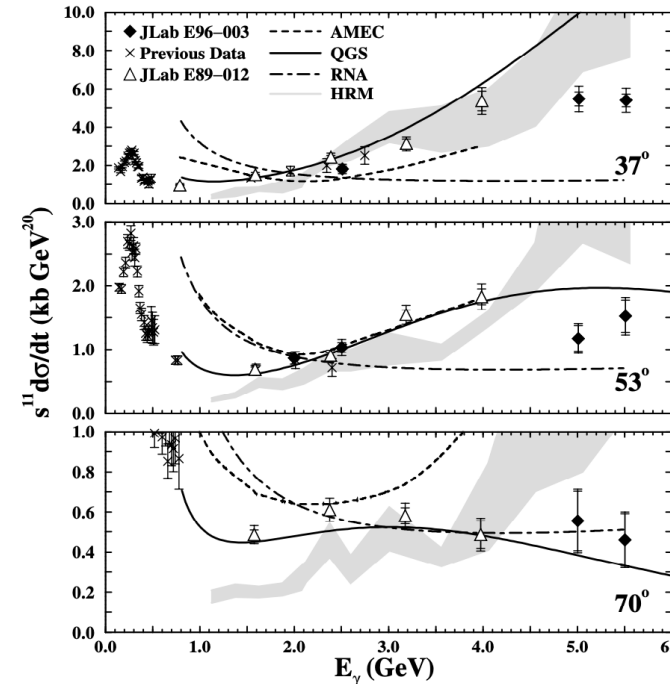


FIG. 2. $s^{11} \frac{d\sigma}{dt}$ vs E_γ for $d(\gamma, p)n$. The present data are shown as solid diamonds. Errors for JLab data are statistical and total errors. All others are statistical only. E89-012 data are shown as open triangles. All other data are shown as crosses and are as presented in Refs. [2,3,22]. The solid line is the QGS calculation [10]. The long-short dashed line is the RNA calculation [11]. The short dashed line is the AMEC [15]. The grey area is the HRM [9].

Summary

- ❖ SBS + BB provide a flexible instrument which is the best choice for many high- z high- Q^2 exclusive reactions.
- ❖ Compact Photon source boosts productivity by 10+ times
- ❖ Approved experimental program is large and additional important physics proposals will be developed.